

# Inhibition of vascular adhesion protein-1 enhances the anti-tumor effects of immune checkpoint inhibitors

Tomonari Kinoshita<sup>1,2</sup> | Mohammad Abu Sayem<sup>1,3</sup>  | Tomonori Yaguchi<sup>1</sup> | Budiman Kharmas<sup>1</sup> | Kenji Morii<sup>1</sup> | Daiki Kato<sup>1,4</sup> | Shigeki Ohta<sup>1</sup> | Yukihiro Mashima<sup>5</sup> | Hisao Asamura<sup>2</sup> | Yutaka Kawakami<sup>1,6</sup>

<sup>1</sup>Division of Cellular Signaling, Institute for Advanced Medical Research, Keio University School of Medicine, Tokyo, Japan

<sup>2</sup>Division of General Thoracic Surgery, Department of Surgery, Keio University School of Medicine, Tokyo, Japan

<sup>3</sup>Department of Biotechnology and Genetic Engineering, Mawlana Bhashani Science and Technology University, Tangail, Bangladesh

<sup>4</sup>Laboratory of Veterinary Surgery, Graduate School of Agricultural and Life Sciences, The University of Tokyo, Tokyo, Japan

<sup>5</sup>Department of Ophthalmology, Keio University School of Medicine, Tokyo, Japan

<sup>6</sup>Department of Immunology, School of Medicine, International University of Health and Welfare, Chiba, Japan

## Correspondence

Yutaka Kawakami and Tomonori Yaguchi, Division of Cellular Signaling, Institute for Advanced Medical Research, Keio University School of Medicine, 35 Shinanomachi, Shinjuku-ku, Tokyo 160-8582, Japan. Emails: yutakawa@keio.jp, yutakawa@iuhw.ac.jp (Y. K.); beatless@rr.ij4u.or.jp (T. Y.)

## Funding information

Japan Agency for Medical Research and Development; Ministry of Education, Culture, Sports, Science and Technology, Grant/Award Number: 15K09783, 19K16808 and 26221005

## Abstract

Modulation of the immunosuppressive tumor microenvironment (TME) is essential for enhancing the anti-tumor effects of immune checkpoint inhibitors (ICIs). Adhesion molecules and enzymes such as vascular adhesion protein-1 (VAP-1), which are expressed in some cancers and tumor vascular endothelial cells, may be involved in the generation of an immunosuppressive TME. In this study, the role of VAP-1 in TME was investigated in 2 murine colon cancer models and human cancer cells. Intraperitoneal administration of the VAP-1-specific inhibitor U-V296 inhibited murine tumor growth by enhancing IFN- $\gamma$ -producing tumor antigen-specific CD8<sup>+</sup> T cells. U-V296 exhibited significant synergistic anti-tumor effects with ICIs. In the TME of mice treated with U-V296, the expression of genes associated with M2-like macrophages, Th2 cells (*Il4*, *Retnla*, and *Irf4*), angiogenesis (*Pecam1*), and fibrosis (*Acta2*, *Loxl2*) were significantly decreased, and the Th1/Th2 balance was increased. H<sub>2</sub>O<sub>2</sub>, an enzymatic product of VAP-1, which promoted the production of IL-4 by mouse Th2 and inhibited IFN- $\gamma$  by mouse Th1 and human tumor-infiltrating lymphocytes, was decreased in tumors and CD31<sup>+</sup> tumor vascular endothelial cells in the TMEs of mice treated with VAP-1 inhibitor. TCGA database analysis showed that VAP-1 expression was a negative prognostic factor in human cancers, exhibiting a significant positive correlation with IL-4, IL4R, and IL-13 expression and a negative correlation with IFN- $\gamma$  expression. These results indicated that VAP-1 is involved in the immunosuppressive TMEs through H<sub>2</sub>O<sub>2</sub>-associated Th2/M2 conditions and may be an attractive target for the development of combination cancer immunotherapy with ICIs.

## KEYWORDS

CTLs, H<sub>2</sub>O<sub>2</sub>, ICIs, immunosuppression, VAP-1 inhibitor

**Abbreviations:** AOC3, amine oxidase, copper containing 3; BLCA, bladder urothelial carcinoma; BRCA, breast invasive carcinoma; ICIs, immune checkpoint inhibitors; IL-4, interleukin-4; KIRC, renal clear cell carcinoma; NK, natural killer; ROS, reactive oxygen species; TAMs, tumor-associated macrophages; TME, tumor microenvironment; VAP-1, vascular adhesion protein-1.

Tomonari Kinoshita and Mohammad Abu Sayem contributed equally to this work.

This is an open access article under the terms of the Creative Commons Attribution-NonCommercial-NoDerivs License, which permits use and distribution in any medium, provided the original work is properly cited, the use is non-commercial and no modifications or adaptations are made.

© 2021 The Authors. *Cancer Science* published by John Wiley & Sons Australia, Ltd on behalf of Japanese Cancer Association.

## 1 | INTRODUCTION

Immunotherapy with ICIs is a promising modality in the treatment of cancers. However, durable responses to the treatment with ICIs, including anti-PD-1/PD-L1 and CTLA4 antibodies, have been observed only in a limited number of patients.<sup>1</sup> To improve the efficacy of ICIs, the mechanisms responsible for the resistance to ICIs therapy need to be understood and overcome. One of the reasons underlying this resistance is the insufficient generation of anti-tumor effector T cells due to the presence of an immunosuppressive tumor microenvironment (TME).<sup>2</sup> The immune-resistance is partly caused by immunosuppressive immune cells, stromal cells, and their secretory molecules and metabolites.<sup>2</sup> Th1 cells producing IFN- $\gamma$  are responsible for activating and regulating the development and persistence of CTLs favoring anti-tumor immunity, whereas Th2 cells producing interleukin (IL)-4 trigger immunosuppressive cascades.<sup>3</sup> Under the influence of IL-4, macrophages differentiate into tumor-promoting M2-like macrophages, generally known as TAMs.<sup>4</sup> NH<sub>3</sub> and H<sub>2</sub>O<sub>2</sub> are signaling metabolites that contribute to tumor progression under various conditions.<sup>5-7</sup>

In this study, we investigated the role of vascular adhesion protein-1 (VAP-1), which is highly expressed in the immunosuppressive TME, and evaluated possible improvements in ICI therapy by targeting VAP-1. VAP-1 is an adhesion molecule involved in the transmigration of immune cells, including myeloid cells,<sup>8</sup> Th2 cells,<sup>9</sup> Treg cells,<sup>10</sup> CD16<sup>+</sup> monocytes,<sup>11</sup> and other inflammatory cells,<sup>12</sup> into the tissues. It has also been reported to contribute to tumor progression through migration of immunosuppressive myeloid cells.<sup>8</sup> VAP-1 is also a topaquinone-containing semicarbazide-sensitive amine oxidase, also known as amine oxidase, copper containing 3 (AOC3), that oxidizes primary amines as per the following reaction:  $R-CH_2NH_2 + H_2O + O_2 \rightarrow R-CHO + NH_3 + H_2O_2$ .<sup>8,13</sup> Under normal conditions, VAP-1 is highly expressed in 3 types of cells in humans: vascular endothelial cells, smooth muscle cells, and adipocytes. Upon inflammation, VAP-1 is expressed in the endothelial cells, and the protein is translocated from cytoplasmic vesicles to the plasma membrane.<sup>8</sup>

The physiological substrate of VAP-1 has not been well defined<sup>8</sup>; however, it is known that VAP-1 can deaminate amino acids such as arginine.<sup>14</sup> Metabolites generated by VAP-1, such as ammonium, aldehyde, and hydrogen peroxide, may negatively influence TAMs at certain concentrations.<sup>15</sup> NH<sub>3</sub> reduces the function of dendritic cells,<sup>16</sup> the viability and activation of lymphocytes, and their ability to secrete cytokines<sup>17</sup> in addition to supporting tumor growth,<sup>5</sup> modulating ion transport,<sup>18</sup> and influencing various immunoregulatory mechanisms.<sup>19</sup> H<sub>2</sub>O<sub>2</sub>, a major component of the ROS, plays several regulatory roles in the TME,<sup>20</sup> including angiogenesis,<sup>21</sup> fibrosis,<sup>22</sup> Th2 skewing,<sup>23,24</sup> M2 skewing,<sup>4,25</sup> and activity suppression of CTL<sup>7,26,27</sup> and NK cells.<sup>7</sup>

VAP-1 was targeted for the treatment of various inflammatory diseases<sup>28-30</sup> using murine models.<sup>31,32</sup> VAP-1 inhibitors and specific monoclonal antibodies were used as treatment remedies in various experimental disease models, including autoimmunity, arthritis,

asthma, ischemia/reperfusion injury, and diabetes.<sup>8</sup> It was reported that both anti-VAP-1 antibodies and VAP-1 inhibitors could reduce the inflammatory responses associated with VAP-1. The expression of VAP-1 in several cancers has been reported.<sup>33-35</sup>

In this study, we evaluated possible modulations of tumor-promoting immunosuppressive TMEs by targeting VAP-1 and improvements in ICI therapy through augmentation of tumor-reactive T cells. We administered a novel VAP-1 inhibitor, U-V296, into 2 murine tumor models, including MC-38/C57BL6 and CT26/BALB/c mice. We observed that U-V296 enhanced the anti-tumor response of tumor antigen-specific CD8<sup>+</sup> T cells accompanied by a decrease in the immunosuppressive Th2/M2-associated TME due to a reduced H<sub>2</sub>O<sub>2</sub> level. In contrast, only a small difference in the number of infiltrating TAMs was observed in our tumor models. Also, a significant synergistic effect was observed between U-V296 and ICIs, including anti-PD-1 and anti-CTLA-4 antibodies. Therefore, VAP-1 may be an attractive target for the development of novel combination cancer immunotherapy with ICIs.

## 2 | MATERIALS AND METHODS

### 2.1 | Mice

Female wild-type C57BL/6 and BALB/c mice, 6-7-wk-old, were purchased from CLEA Japan, Inc. Murine NOG (NOD/Shi-SCID, IL-2R $\beta$  null) mice deficient in MHC class I and II were also used to examine the effect of the immune system during the anti-tumor response.<sup>36</sup> All mice were maintained under specific pathogen-free conditions and used for the study upon approval by the Animal Care and Use Committee of the Keio University School of Medicine.

### 2.2 | Cell lines and transplantation

MC-38 and CT26 (both murine colon carcinoma cell lines) were cultured in RPMI 1640 medium (Gibco Invitrogen) supplemented with 10% FCS, 100 U/mL of penicillin, and 100  $\mu$ g/mL of streptomycin. An area on their flanks was shaved into which tumor cells ( $5 \times 10^5$  cells per mouse) contained in PBS (100  $\mu$ L) were subcutaneously injected. Subsequent growth of the tumor was recorded by measuring its dimensions using an electronic caliper. The tumor sizes were measured every 3 d, and their volumes were estimated using the following formula:  $V = 0.5 \times (\text{shortest diameter})^2 \times (\text{longest diameter})$ .

### 2.3 | Treatment with the VAP-1 inhibitor

Tumors on the injected areas were palpable on the fifth day post subcutaneous inoculation of the cancer cells. An inhibitor of VAP-1 (U-V296), developed by Sucampo Pharmaceuticals, was intraperitoneally administered with daily doses of 10 mg/kg. Vehicle (physiological saline) injections served as a negative control. The first day of treatment

was defined as day 0. After 2 wk of initial injection (day 15), the tumors were removed, washed with sterile RPMI 1640, cut into fragments of 1 to 3 mm dimensions with a pair of scissors, and placed in solutions of type IV collagenase (1.4 mg/mL; Sigma) and DNase (0.3 KU/mL; Sigma). The tumor fragments, therefore collected in the flasks, were incubated under conditions of slow and continuous shaking at 37°C for 30 min to form suspensions. These cell suspensions were then passed through nylon filters and used for further analysis.

## 2.4 | Detection of the tumor antigen-specific T cell response through the release of mouse IFN- $\gamma$ and cytotoxicity assay

Single-cell suspensions of draining lymph nodes (axillary and inguinal, present on the same side of the transplanted tumors) and spleens from each mouse were cultured in RPMI 1640 medium supplemented with 10% FBS. These were stimulated using 1  $\mu$ g/mL of the tumor-specific peptides gp70 or AH-1 in MC-38 or CT26 cell lines, respectively, followed by irradiation (32 Gy) of the syngeneic splenocytes for 5 d. Tumor-infiltrating CD8<sup>+</sup> T cells from the digested tumor cells were isolated using CD8a (Ly-2) MicroBeads and autoMACS (Miltenyi Biotec KK) and cultured for 2 d with the tumor Ag as mentioned above. These cultured CD8<sup>+</sup> T cells were harvested, washed, and incubated with EL-4 cells in the presence of gp70 or AH-1 at different concentrations of 0, 0.01, 0.1, or 1  $\mu$ g/mL for 16–20 h ( $2 \times 10^5$  T cells and  $2 \times 10^5$  EL-4 cells/200  $\mu$ L/well). Then, the concentration of IFN- $\gamma$  was determined using ELISA (mouse IFN- $\gamma$  CytoSet; Life Technologies, and BD OptEIA; BD Biosciences, respectively). Mouse IFN- $\gamma$  was detected in the range of 31.3–1000 pg/mL.  $\beta$ -Galactosidase ( $\beta$ -gal) was used as a negative control for the tumor-specific peptide. For target cells killing assay, EL-4 cells pulsed with peptide were labeled with 5  $\mu$ mol/L Calcein-AM (eBioscience) and co culture with T cells. Fluorescence of calcein released from the dead cells were measured.

## 2.5 | Treatment with ICIs (anti-PD-1 and anti-CTLA-4) and depletion of immune cells

Mice were administered with the following antibodies purchased from Bio X Cell on days 0, 3, and 6: anti-PD-1, anti-CTLA-4, anti-mouse CD4, anti-mouse CD8, and anti-mouse NK1.1/NK1.2, each at a dosage of 200  $\mu$ g/body. As a control treatment, each antibody isotype was administered intraperitoneally on the same day as that of the test after implantation of the tumor.

## 2.6 | Transcriptome analysis of mouse tumor tissue with or without VAP-1 inhibition and TCGA analysis

Total RNA was isolated from 8 samples of the mouse tumor ( $n = 4$  for both vehicle and the treatment group, U-V296) using a column-based method (Qiagen RNeasy; Qiagen, Hilden, Germany). Purity

and integrity of the RNA were evaluated using an ND-1000 spectrophotometer (NanoDrop) and Agilent 2100 Bioanalyzer (Agilent Technologies). RNA labeling and hybridization were carried out using the Agilent One-Color Microarray-Based Gene Expression Analysis protocol (Agilent Technology, v.6.5, 2010). Briefly, 100 ng of total RNA from each sample was linearly amplified and labeled using Cy3-dCTP. The labeled cRNAs were purified using an RNeasy Mini Kit (Qiagen). The concentration and specific activities of the labeled cRNAs (pmol Cy3/ $\mu$ g of cRNA) were measured using a NanoDrop ND-1000 (NanoDrop). Each labeled cRNA, 600 ng in quantity, was fragmented by treating with 5  $\mu$ L of a 10 $\times$  blocking agent and 1  $\mu$ L of 25 $\times$  fragmentation buffer, followed by heating at 60°C for 30 min. Finally, 25  $\mu$ L of a 2 $\times$  GE hybridization buffer was added to dilute the labeled cRNA, after which 40  $\mu$ L of the hybridization solution was dispensed into a gasket slide and assembled with the Agilent SurePrint G3 Mouse GE 8X60K, V2 Microarrays (Agilent Technologies). The slides were incubated for 17 h at 65°C in an Agilent hybridization oven. Then, they were washed at room temperature using the Agilent One-Color Microarray-Based Gene Expression Analysis protocol (Agilent Technology, V6.5, 2010). The hybridized array was immediately scanned using an Agilent Microarray Scanner D (Agilent Technologies).

The microarray results were extracted using the Agilent Feature Extraction software v.11.0 (Agilent Technologies) and normalized using gene expression and functional profiling analysis suite, Babelomics 4,<sup>37</sup> followed by the Agilent one-channel normalization. After normalization, the data set was evaluated and reduced. Replicates of probes with lower variance and those without gene names were deleted. Furthermore, probes for microRNAs were not included in the analysis. As a result, a final set of 23 599 (out of 59 305) expression values was obtained. Unsupervised hierarchical cluster analysis was performed, and the data were visualized using Cluster3 and TreeView 3.0, respectively. Correlation analysis of TCGA data were performed using the online tool GEPIA 2 and GraphPad Prism 6.

## 2.7 | In silico immune cell-type deconvolution using the gene expression data

We used the normalized (RPKM) gene expression values as an input in CIBERSORT for the in silico estimation of the relative abundance of immune cell populations in the samples.<sup>38</sup> We used the immune cell signature matrix produced specifically for mouse tissue as the signature gene file.<sup>39</sup> The number of permutations applied was 100 (default).

## 2.8 | Measurement of H<sub>2</sub>O<sub>2</sub> as an indicator of the enzymatic activity of VAP-1

The Amplex Red assay (Thermo Fisher) was used to measure the VAP-1 activity in lysates and CD31<sup>+</sup> cells of the tumors. Briefly, the

tumor tissue was lysed using 1.0% NP-40 (Sigma) in PBS, and the total protein content from this lysate was calculated using a colorimetric assay employing the standard protein bovine serum albumin (Bio-Rad) and the Coomassie brilliant blue reagent. Then, 1 mg of clarified supernatant from the samples was incubated with or without U-V296, to which benzylamine (a substrate of VAP-1) was added.  $H_2O_2$  was kinetically generated after the addition of the Amplex Red detection mixture, which was detected by measuring the fluorescence of the samples using 2104 EnVision® Multilabel Plate Readers. The specific activity of VAP-1 was measured by subtracting the emission values read for the control wells without the substrate.<sup>32</sup> A Krebs-Ringer phosphate glucose (KRPBG) buffer (comprising 145 mmol/L NaCl, 5.7 mmol/L sodium phosphate, 4.86 mmol/L KCl, 0.54 mmol/L  $CaCl_2$ , 1.22 mmol/L  $MgSO_4$ , and 5.5 mmol/L glucose; pH 7.35) was used to detect its activity in  $CD31^+$  cells.<sup>40</sup>  $CD31^+$  cells were magnetically sorted and used instead of the tumor lysate and processed in accordance with the same method as described above.

## 2.9 | Effect of extracellular $H_2O_2$ on the production of cytokines by T cells

Mouse Th1 and Th2 cells were generated in vitro using a method published previously.<sup>41</sup> Briefly, naïve  $CD4^+$  cells were sorted using the  $CD62L^+CD4^+$  Isolation Kit from Miltenyi Biotec (USA). These  $CD4^+$  cells were stimulated using a plate coated with the anti-CD3 (2  $\mu$ g/mL) and soluble anti-CD28 antibodies (2  $\mu$ g/mL) in the presence of 3.33 ng/mL, 10  $\mu$ g/mL, and 10  $\mu$ g/mL of IL-12 (Peprotech), anti-IL-4 for Th1 or IL-4 (Peprotech), and anti-IFN- $\gamma$  for Th2 cells, respectively, in RPMI 1640 medium supplemented with 10% FCS, 100 U/mL penicillin, 100  $\mu$ g/mL streptomycin, 55 mmol/L  $\beta$ -mercaptoethanol, Na-pyruvate, and nonessential amino acids (NEAA, Gibco, Life Technologies). To assess the effect of  $H_2O_2$  on the production of cytokines by T cells, Th1 or Th2 cells were re-stimulated using a plate coated with the anti-CD3 antibody (2  $\mu$ g/mL) and soluble anti-CD28 antibody (2  $\mu$ g/mL) and cultured overnight in the presence or absence of 100  $\mu$ mol/L  $H_2O_2$  (Sigma) and IL-2 (50 IU/mL) or PMA + ionomycin. Na-pyruvate was added to neutralize the effect of  $H_2O_2$ . After incubation, the supernatant was collected, and the levels of IFN- $\gamma$  or IL-4 were measured using ELISA (BD OptEIA, BD Biosciences). Human melanoma-derived T cells were cultured using a high dose of IL-2<sup>42</sup> and then activated using PMA (50 ng/mL) and ionomycin (1  $\mu$ g/mL) for 4 h in the presence or absence of an indicated amount of  $H_2O_2$ .

## 2.10 | Immunohistochemistry

The formalin-fixed, paraffin-embedded specimens were cut into sections of 5- $\mu$ m thickness. The tissue sections were microwaved with the antibody of interest in a medium containing 10 mmol/L citrate buffer at pH 6.0 to facilitate heat-induced epitope retrieval. Each slide was incubated overnight at 4°C with CD8 primary Abs at 1:50 dilution (Santa Cruz Biotechnology). These were further

incubated with the goat anti-rat HRP MAX-PO (R) for 30 min at room temperature to enable visualization of the bound primary antibody. The specimens were visualized using 2% 3,3'-diaminobenzidine in 50 mmol/L Tris buffer (pH 7.6) containing 0.3%  $H_2O_2$ . In some cases, stained tissue sections were scanned by NanoZoomer (Hamamatsu Photonics KK) and counted using TissueQuest cell analysis software (TissueGnostics GmbH).

## 2.11 | Statistical analysis

All results were expressed as the mean  $\pm$  SD. The data were subjected to statistical analyses (unpaired Student *t* test) to determine the differences among the means of the experimental, treatment and control groups. Differences were considered to be statistically significant at values of  $P < .05$ .

# 3 | RESULTS

## 3.1 | VAP-1 inhibition suppresses tumor growth in a $CD8^+$ T cell-dependent manner in 2 murine tumor models

To investigate the role of VAP-1 in the tumor immune microenvironment, a novel VAP-1 inhibitor, U-V296, was intraperitoneally administered to mice with palpable tumors at day 5 (Figure 1). The VAP-1 inhibitor significantly reduced tumor growth in both murine colon cancer models, MC-38/C57BL6 (Figure 1A) and CT26/BALB/c (Figure 1B). The inhibition of tumor growth was not the result of a direct anti-tumor effect of the inhibitor because it was not toxic to the MC-38 (Figure S1A) or CT26 tumor cell lines in vitro (data not shown) at a concentration of up to 10  $\mu$ g/mL. Suppression of tumor growth by U-V296 was not observed in immunodeficient NOD/Shi-SCID/IL2R $\gamma$ null (NOG) mice (Figure 1C). Depletion of  $CD8^+$  T cells, but not  $CD4^+$  T or NK cells, reversed the anti-tumor effect of the VAP-1 inhibitor (Figure 1D-F). These results indicated that the inhibition of VAP-1 led to anti-tumor effects through the induction of tumor-specific  $CD8^+$  cytotoxic T cells.

## 3.2 | Enhancement of IFN- $\gamma$ production and cytotoxic activity of tumor antigen-specific $CD8^+$ T cells following the administration of U-V296

We then evaluated the effect of the VAP-1 inhibitor on the induction of tumor antigen-specific T cells in vivo. The induction of T cells specific for the immunodominant antigen gp70 of MC-38 tumors was examined using an IFN- $\gamma$  release assay. The production of IFN- $\gamma$  by gp70-specific T cells in the tumors, spleens, and draining lymph nodes was significantly increased by the inhibition of VAP-1 (Figure 2A-C). T cell cytotoxic genes, such as *Prf1*, *Gzma*, *Gzmb*, and *Gzmc*, were increased in the TME (Figure 2D). The cytotoxic activity of splenic T cells against EL4 cells pulsed with gp70 peptide was also

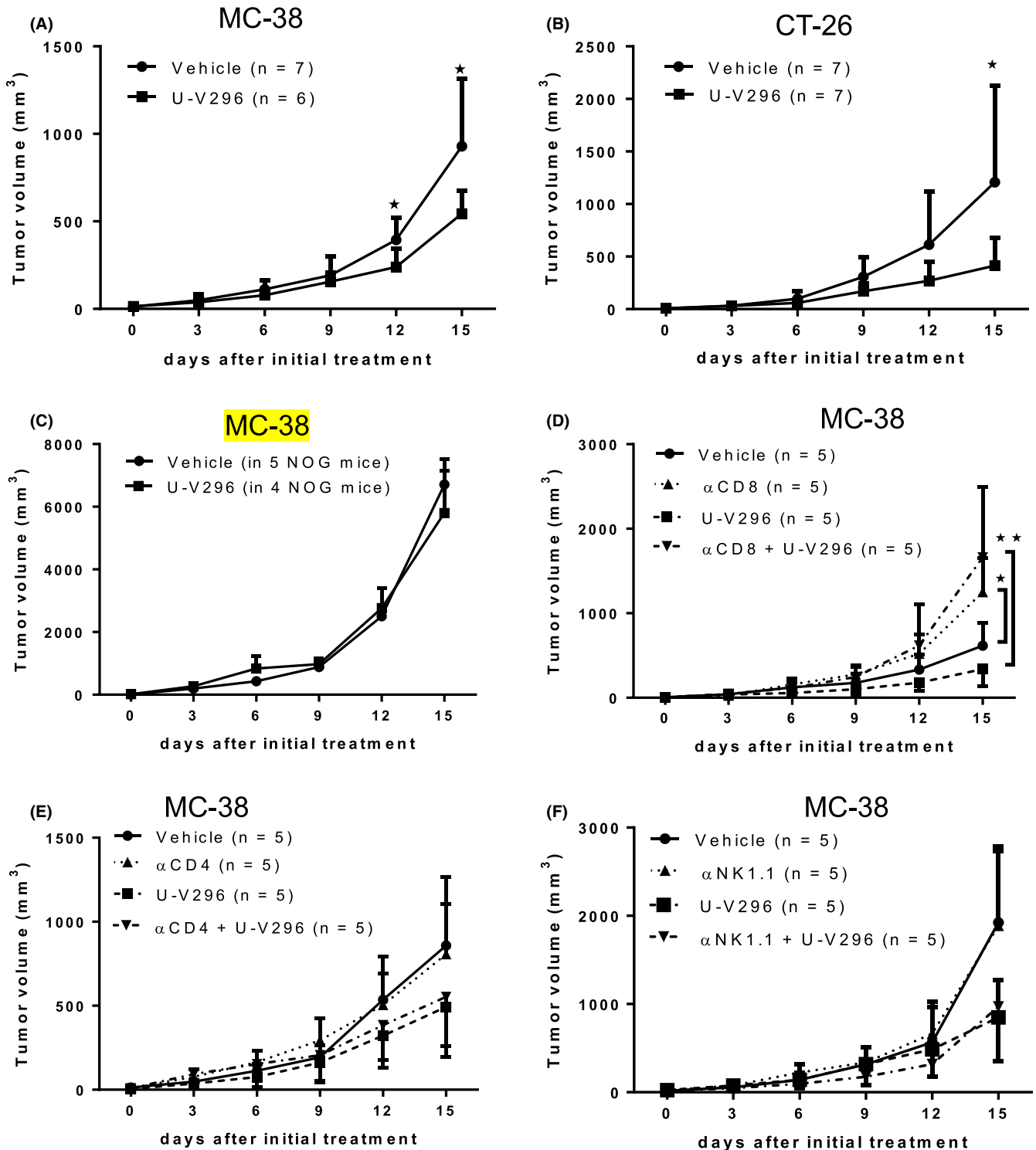


**FIGURE 1** Intraperitoneal injection of U-V296 inhibited tumor growth in the MC-38 and CT26 murine tumor models. Mononuclear cells were collected from tumors, draining lymph nodes, and spleens for further analysis 15 d after U-V296 injection. The size of the tumors was measured at indicated time points. A, B, U-V296 treatment inhibits tumor growth in the MC-38 (A) and CT26 (B) murine tumor models. C, A non-significant anti-tumor effect was observed in MC-38 cells upon U-V296 treatment of NOG mice. D, Depletion of CD8<sup>+</sup> T cells using an antibody ( $\alpha$ CD8) reversed the anti-tumor effect of U-V296. E, F, U-V296 treatment inhibited tumor growth in MC-38 cells, regardless of the administration of the antibodies for anti-CD4 ( $\alpha$ CD4) or anti-NK1.1/NK1.2 ( $\alpha$ NK1.1). \* $P < .05$ ; \*\* $P < .01$

enhanced by VAP-1 inhibition (Figure 2E). Similarly, the production of IFN- $\gamma$  by AH-1-specific T cells was significantly increased by the inhibition of VAP-1 in the CT26/BALB/c murine model (Figure S1B).

However, no significant changes in the immune cells within the tumors, including macrophages, MDSCs, CD4, CD8, B-cells, NK cells, and neutrophils, were observed by VAP-1 inhibition (Figure S2A,B).

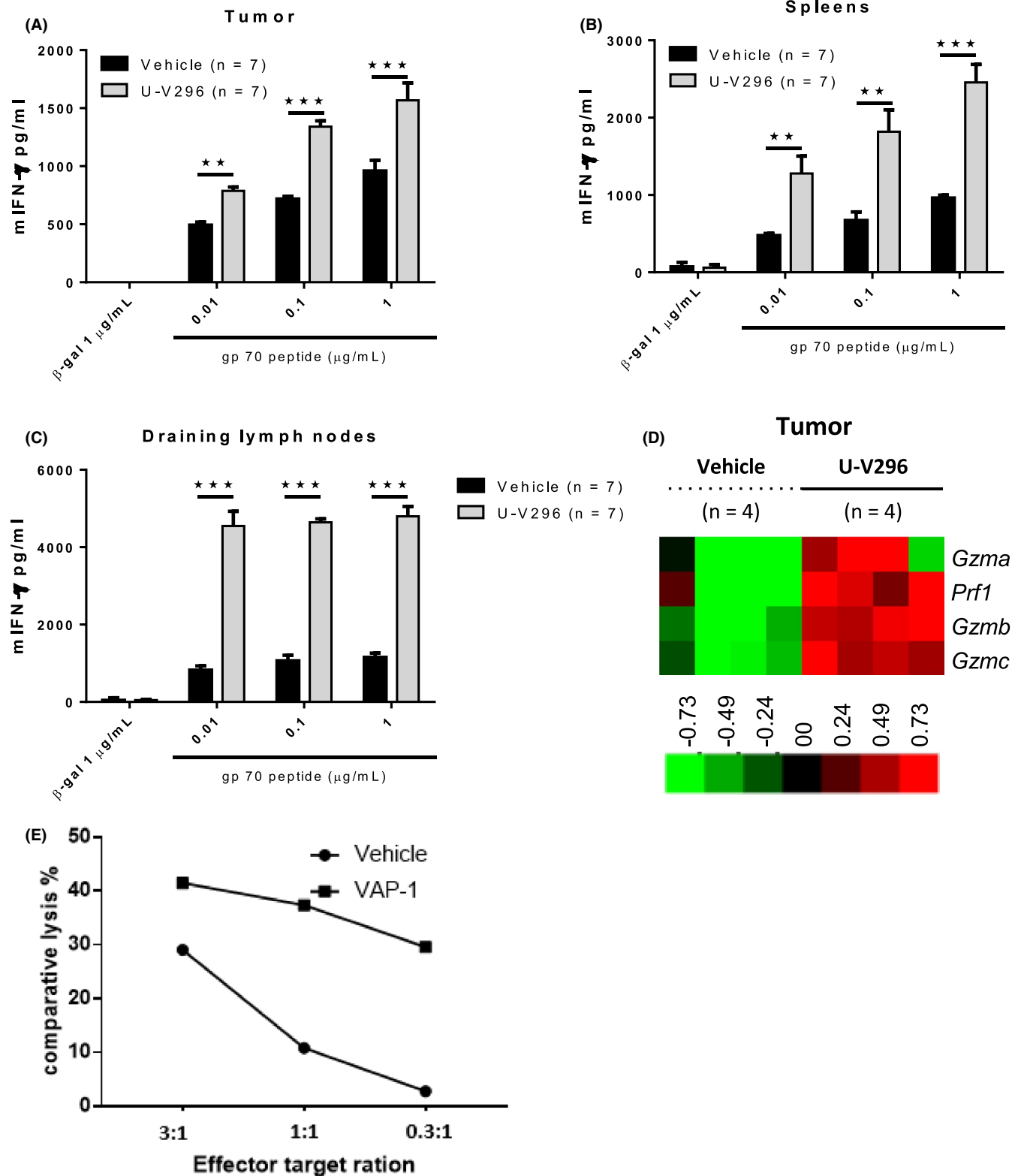


**FIGURE 2** Inhibition of VAP-1 enhanced the production of IFN- $\gamma$  by CD8<sup>+</sup> T cells and cytolytic genes in the TME. A-C, Enhanced production of IFN- $\gamma$  in response to EL-4 cells and the MC-38 tumor antigen gp70 was observed in CD8<sup>+</sup> T cells isolated from the tumor tissues, spleens, and draining lymph nodes. The cells were pooled from 7 mice, cultured for a short period with the gp70 peptide, and subjected to ELISA in replicates. Representative data from 4 experiments with similar results are shown. D, Microarray analysis revealed that the inhibition of VAP-1 upregulated the expressions of cytolytic genes (*Prf1*, *Gzma*, *Gzmb*, and *Gzmc*) in TME. E, Inhibition of VAP-1 enhanced cytotoxic activity of tumor antigen-specific T cells. \*\* $P < .01$ ; \*\*\* $P < .001$

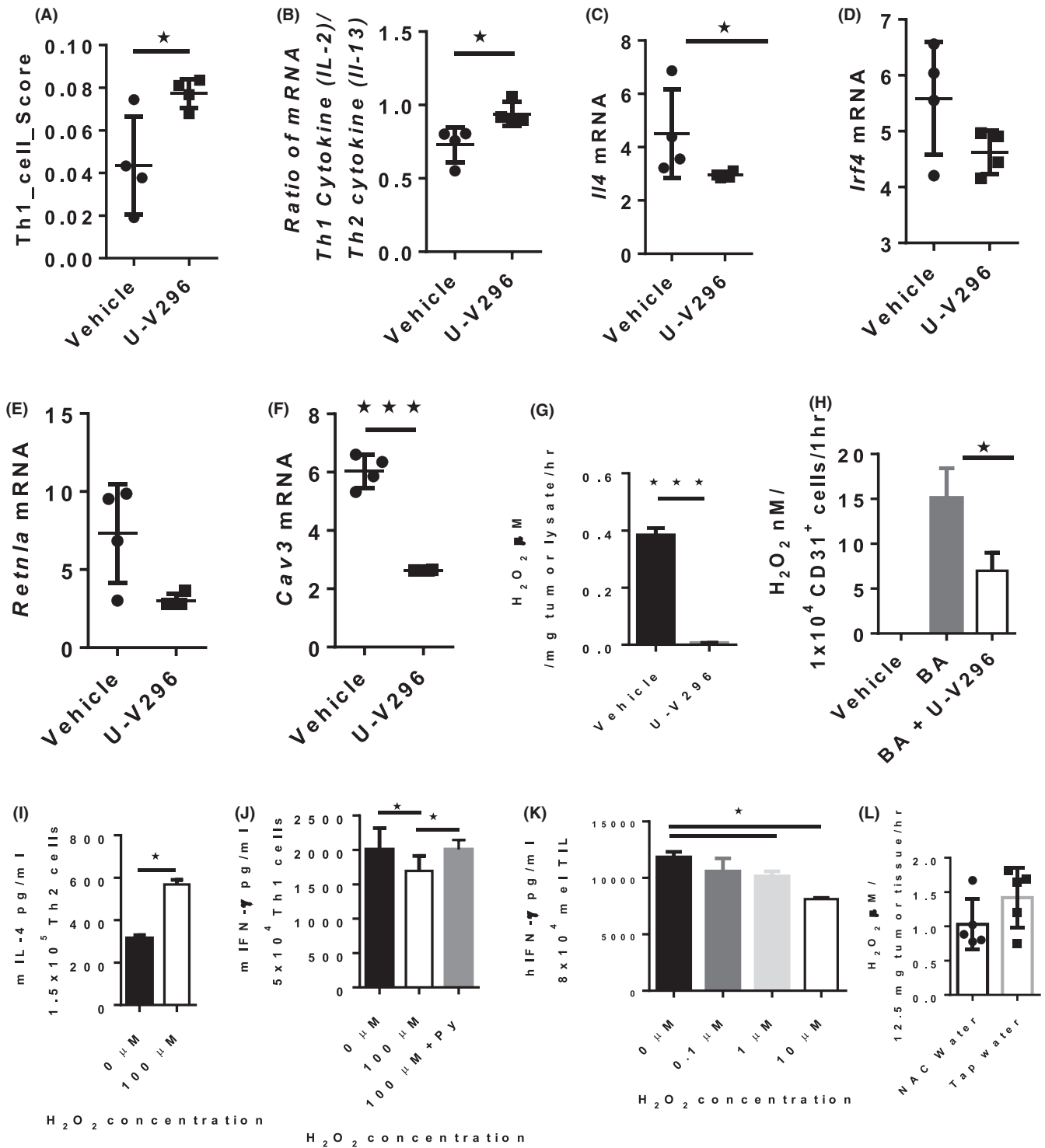


**FIGURE 3** Th1-associated phenotype is favored over that of Th2 or M2 upon inhibition of VAP-1. A-F, VAP-1 inhibition enhanced the Th1 score, calculated using CIBERSORT, and Th1/Th2 cytokine ratio and reduced the gene expression of IL-4, M2-associated transcription factor *Irf4*, M2-associated marker *Retnla*, and *Cav3*. G, U-V296 inhibited the production of H<sub>2</sub>O<sub>2</sub> in the tumor lysate derived from MC-38 tumor-bearing mice. H, U-V296 inhibited the production of H<sub>2</sub>O<sub>2</sub> in CD31<sup>+</sup>-enriched endothelial cells containing VAP-1; BA: benzylamine (substrate of VAP-1). I, H<sub>2</sub>O<sub>2</sub> increased the production of IL-4 by mouse Th2 cells upon stimulation. J, Higher concentrations of H<sub>2</sub>O<sub>2</sub> inhibited the production of mIFN-γ by mouse Th1 cells upon stimulation and the inhibition was cancelled by the addition of Napyruvate (Py). K, H<sub>2</sub>O<sub>2</sub> inhibited the production of hIFN-γ by human melanoma infiltrated T lymphocytes (mel TIL) cultured ex vivo and stimulated using PMA and ionomycin for 4 h. 3L, Addition of N-acetyl cysteine (NAC) in drinking water reduces H<sub>2</sub>O<sub>2</sub> content in tumor tissues. \*P < .05; \*\*\*P < .001

### 3.3 | Inhibition of VAP-1 enhances the Th1 response and inhibits the immunosuppressive Th2/M2 responses by decreasing the H<sub>2</sub>O<sub>2</sub> level in tumors

To investigate whether the enhanced anti-tumor effect was caused by improving the immunosuppressive TME, we performed cDNA microarray analysis on murine tumors after various treatments. The relative abundance of various immune cells was evaluated in silico using CIBERSORT, revealing that the Th1 score (Figure 3A) and Th1/Th2 cytokine ratio (IL-2/IL-13) were increased upon VAP-1 inhibition (Figure 3B), whereas the expression of the genes for IL4 (*Il-4*), transcription factor IRF4 (*Irf4*), and surface marker Fizz1 (*Retnla*), which are associated with the Th2/M2 phenotype, was significantly decreased (Figure 3C-E).

The ROS-induced expression of *Cav3*, a gene encoding the protein caveolin-3,<sup>43,44</sup> was also significantly reduced in U-V296-treated mice (Figure 3F), indicating that H<sub>2</sub>O<sub>2</sub> was involved in the modulation of the immune status of our tumor models. It has been reported that ROS is involved in angiogenesis<sup>21</sup> and fibrosis<sup>22</sup>; we found that genes related to angiogenesis (*Pecam1* encoding CD31 expressed on endothelial cells) and fibrosis (*Col1a1* encoding collagen type 1, *Acta2* encoding SMA, and *Loxl2* encoding Lysyl oxidase homolog 2) were decreased following VAP-1 inhibition (Figure S3A-G).<sup>12</sup> We also found that the production of H<sub>2</sub>O<sub>2</sub> was almost completely inhibited in tumor lysates (Figure 3G) and CD31<sup>+</sup> endothelial cells (primary cells highly expressing VAP-1) isolated from excised tumors (Figure 3H) from mice treated with the VAP-1 inhibitor. These results suggested that the VAP-1 inhibitor improved the immunosuppressive TME by reducing the VAP-1-mediated generation of H<sub>2</sub>O<sub>2</sub> in various cells, including tumor vasculature endothelial and tumor cells.

The increased production of IL-4 by Th2 cells and decreased production of IFN- $\gamma$  by Th1 cells in the presence of H<sub>2</sub>O<sub>2</sub> have previously been reported.<sup>23</sup> We, therefore, examined the in vitro effects of H<sub>2</sub>O<sub>2</sub> on Th1 and Th2 cells using mouse splenocytes (Figure S4A,B). We confirmed a marked increase in the productions of IL-4 by Th2 cells (Figure 3I) and a decrease in IFN- $\gamma$  production by Th1 cells (Figure 3J) in the presence of H<sub>2</sub>O<sub>2</sub>, that is cancelled by the addition of a scavenger of H<sub>2</sub>O<sub>2</sub>, Na-pyruvate. A similar phenomenon was also observed using ex vivo cultured human melanoma tumor-infiltrating lymphocytes (TILs) (Figure 3K). These results suggested that the inhibition of VAP-1 reduced the production of H<sub>2</sub>O<sub>2</sub>, leading to a decrease in IL-4 production and the related Th2/M2-associated phenotype, improvement of the Th1/Th2 balance, and enhancement of tumor antigen-specific CD8<sup>+</sup> T cell induction.

### 3.4 | Expression of VAP-1/AOC3 correlates positively with the expression of H<sub>2</sub>O<sub>2</sub>-sensitive caveolin and Th2/M2-related genes but negatively with the prognosis of patients with cancers

We evaluated the role of VAP-1/AOC3 in human cancers. TCGA database analysis revealed that VAP-1/AOC3 was a negative prognostic

factor in 3 cancer types: colorectal, renal, and urothelial cancer (Figure 4A). We also found that the gene expression of AOC3/VAP-1 was positively correlated with that of caveolin-1-3, IL4, IL4R, and IL-13, but negatively correlated with that of IFN- $\gamma$  in colorectal, renal, and urothelial cancers (Figures 4B and S4C). These results indicated that VAP-1 might also be involved in the H<sub>2</sub>O<sub>2</sub>-mediated immunosuppressive Th2/M2 phenotype in human cancers.

### 3.5 | Significant synergistic anti-tumor effect between the VAP-1 inhibitor and ICIs

We tested whether the VAP-1 inhibitor-mediated anti-tumor effect is potentiated by the combination with ICI therapy, including anti-PD-1, anti-CTLA-4, and both PD-1 and CTLA-4 antibodies. Significant synergistic effects were observed in combination with anti-CTLA-4 (Figure 5A) or anti-PD-1 antibodies (Figure 5B). Tumor regrowth after initial inhibition was observed in all mice after doublet therapies. However, upon triplet therapy with U-V296, anti-CTLA-4, and anti-PD-1 antibodies, 3 out of 5 mice were completely tumor-free (Figure 5C-E), although the accumulation of CD8<sup>+</sup> T cells in tumors was not significantly changed by VAP-1 inhibition in the ICI combination settings (Figure 5F). These results indicated that targeting VAP-1 is an attractive strategy for combination cancer immunotherapy with ICIs.

## 4 | DISCUSSION

In this study, we showed that VAP-1 expressed in cancer and tumor vascular endothelial cells was involved in the immunosuppressive TME through H<sub>2</sub>O<sub>2</sub>-associated Th2/M2-related cascades. The VAP-1 inhibitor U-V296 augmented the induction of tumor antigen-specific CD8<sup>+</sup> T cells and synergized with ICIs (anti-PD-1 and CTLA-4 antibodies).

It has previously been reported that VAP-1 modulates the transmigration of neutrophils, granulocytes, macrophages, and lymphocytes under various inflammatory conditions, including those associated with tumors.<sup>8</sup> Knockout of VAP-1 expression and pharmacological inactivation or inhibition of VAP-1 reportedly suppress tumor growth by inhibiting the infiltration of inflammatory myeloid cells (eg, TAMs), angiogenesis, and fibrosis.<sup>8,12,25,31,32</sup> We observed a similar reduction in tumor growth in our 2 murine tumor models using the VAP-1 inhibitor U-V296. The U-V296-mediated anti-tumor effect depended on IFN- $\gamma$  producing tumor antigen-specific cytotoxic CD8<sup>+</sup> T cells. VAP-1 inhibition led only to minimal differences in the number of infiltrated immunosuppressive cells, such as TAMs, MDSCs, B-cells, and NK cells. However, gene expression analysis in tumors from VAP-1-treated mice revealed functional changes in tumor-infiltrating immune cells, including an increase in the Th1/Th2 ratio and a decrease in the expression of IL-4 and other genes related to the Th2-M2-phenotype, angiogenesis, and fibrosis. IL4 triggers the differentiation of alternatively activated macrophages (M2-like macrophages), which contribute

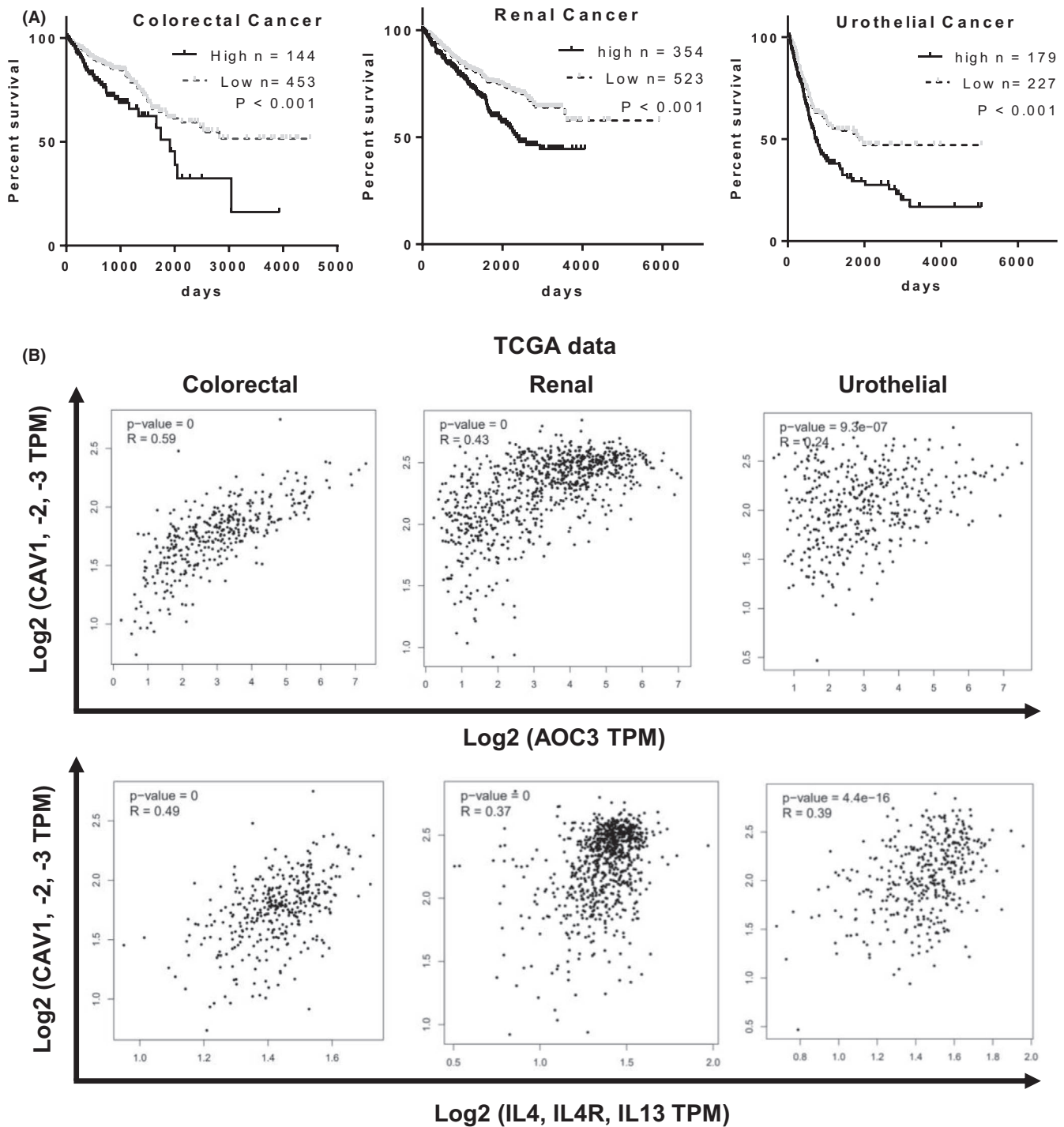
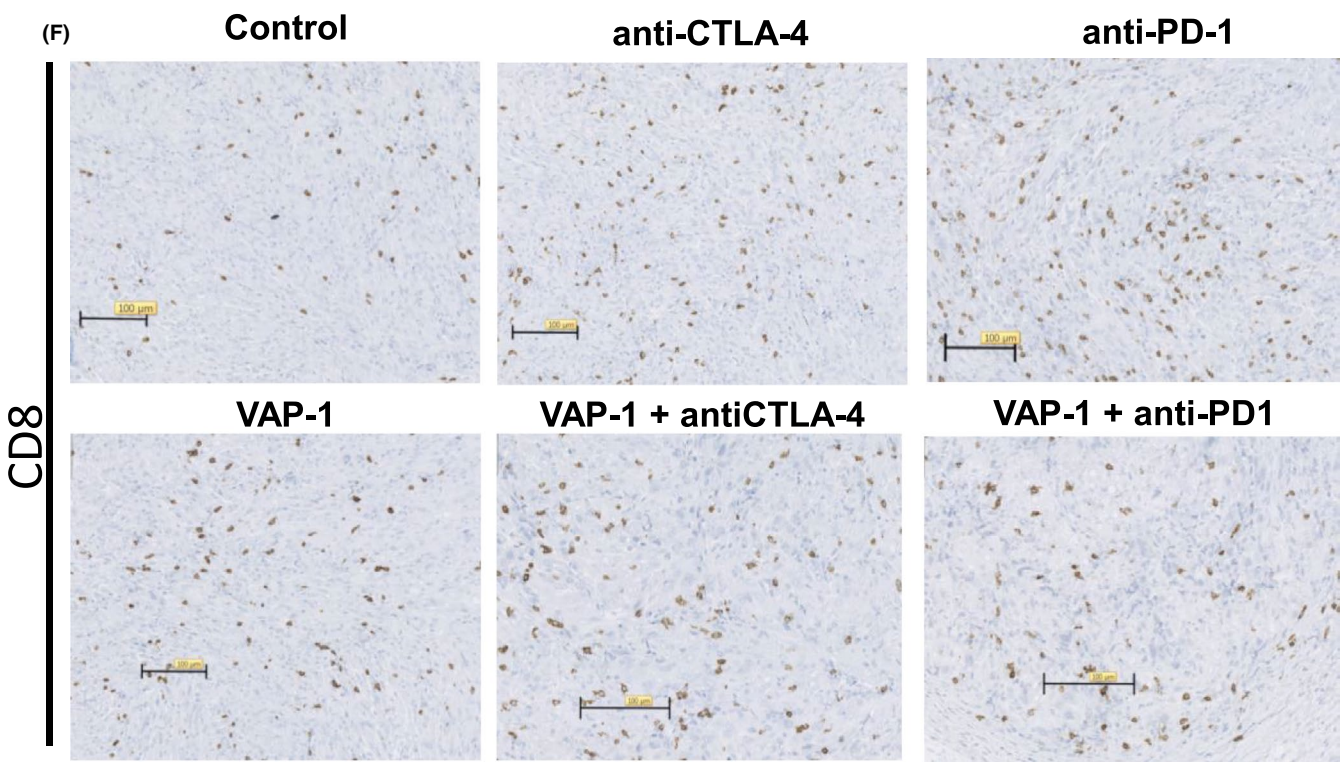
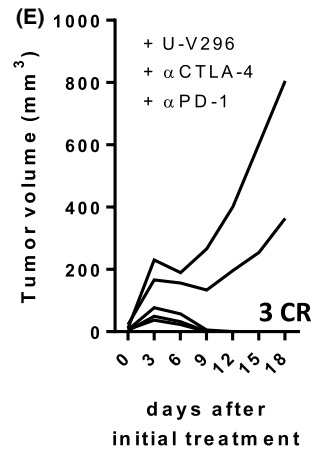
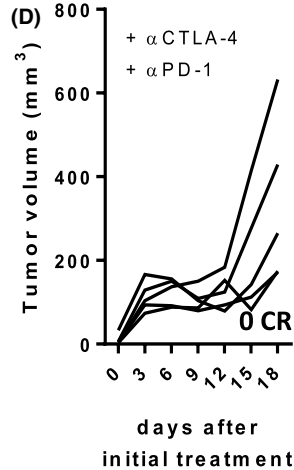
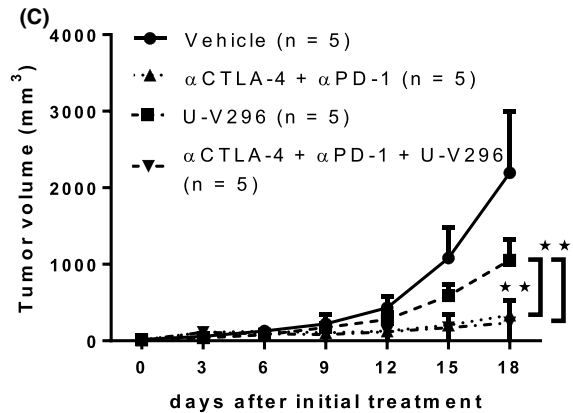
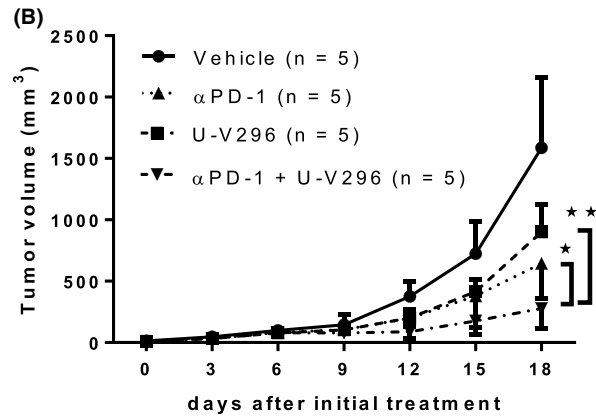
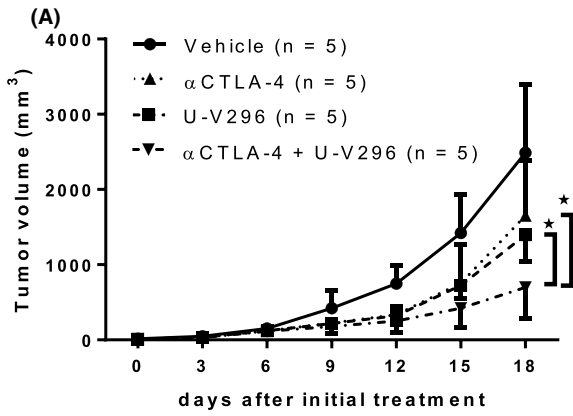


**FIGURE 4** AOC3, an  $H_2O_2$ -sensitive protein, was associated with poor prognosis and Th2-associated gene expression in multiple human cancers. A, AOC3 expression is a negative prognostic factor in colorectal, renal, and urothelial cancer. B, CAV1, -2, -3 expression levels were positively correlated with AOC3 and IL4/IL4R/IL13 expression in colorectal, renal, and urothelial cancer

to inflammatory angiogenesis and immune evasion of tumor cells. VAP-1 was reported to mediate the infiltration of M2 macrophages into inflammatory sites.<sup>25</sup> The transcription factor IRF4 is involved in the IL-4-dependent induction of a set of M2-specific marker genes such as *FIZZ1* (*Retnla*).<sup>45</sup> Enhanced expression of IRF4 and *Retnla* was observed in the TMEs of mice following VAP-1 inhibitor administration.

Regarding the mechanism underlying the VAP-1-induced immunosuppression (with a Th2/M2 immune cell phenotype), our gene expression analysis revealed a decreased gene expression of *Cav3*, which is induced by ROS,<sup>43,44,46</sup> in U-V296-treated tumors.  $H_2O_2$  is the enzymatic product of VAP-1 and was reported to affect the function of T cells negatively.  $H_2O_2$  derived from activated granulocytes suppressed the function of T cells in patients with advanced



cancer.<sup>26</sup> In addition, extracellular H<sub>2</sub>O<sub>2</sub> can reduce the anti-tumor function of T cells, possibly through the downregulation of the CD3 ζ-chain.<sup>6,27</sup> In this study, treatment of tumor lysates or endothelial

cells with the VAP-1 inhibitor reduced the production of H<sub>2</sub>O<sub>2</sub>, indicating that the function of T cells might be improved partly by a decrease in the H<sub>2</sub>O<sub>2</sub> level.

**FIGURE 5** Combination of U-V296 and ICIs such as anti-PD-1 and anti-CTLA4 synergistically improved the anti-tumor response. A, B, Doublet therapies (A, U-V296 +  $\alpha$ CTLA-4; B, U-V296 +  $\alpha$ PD-1) exhibited synergistic anti-tumor effects. C-E, Triplet therapy (U-V296 +  $\alpha$ CTLA-4 +  $\alpha$ PD-1) strongly suppressed tumor growth. D, E, All tumors regrew within 2 wk after initial administration of the  $\alpha$ CTLA-4/ $\alpha$ PD-1 doublet therapies, whereas 3 out of 5 tumors disappeared without relapse upon application of the triplet therapy. F, Accumulation of CD8<sup>+</sup> T cell in tumors were not significantly increased by VAP-1 inhibition in the ICI combinations therapies. \* $P < .05$ ; \*\* $P < .01$

Several reports have discussed the role of H<sub>2</sub>O<sub>2</sub> in immunosuppressive TMEs. It was reported that H<sub>2</sub>O<sub>2</sub> inhibited the release of IL-4 from various immune cells, including Th2<sup>23</sup> and mast cells,<sup>47</sup> and induced a Th2-dominant response in mice by increasing the molecular ratio of interleukin-12 p40/p70.<sup>24</sup> The ROS inhibitor butylated hydroxyanisole (BHA) inhibited M2 polarization mediated by GM-CSF or M-CSF but not that by M1.<sup>4</sup> The knockout of ROS-producing enzymes was reported to result in the development of a Th1 phenotype.<sup>6</sup> Anti-VAP-1 antibodies were found to effectively inhibit the rolling of Th2 cells in the liver sinusoids, but they did not affect that of Th1 cells in a concanavalin A-induced liver injury model.<sup>9</sup> These reports indicated that H<sub>2</sub>O<sub>2</sub> produced by VAP-1 induced IL4-related Th2-M2 responses, thereby inhibiting the Th1 response. In this study, we showed that U-V296 reduced H<sub>2</sub>O<sub>2</sub> production in tumor lysates in vitro and enhanced the Th1 cell score and Th1/Th2 cytokine balance in vivo, accompanied by decreased expression of *Il-4*, *Irf4*, and *Retnla*. The possible role of the VAP-1 substrate polyamine and the VAP-1 product NH<sub>3</sub><sup>8</sup> was also evaluated in this study. Polyamines are essential for the growth and function of various normal cells and are dysregulated in TMEs.<sup>48</sup> NH<sub>3</sub> reportedly affects dendritic cells to stimulate lymphocytes in tumors.<sup>16</sup> No differences in the production of NH<sub>3</sub> and the major polyamine-metabolizing enzymes were observed in our tumor models (data not shown). These results indicated that VAP-1 inhibition augmented anti-tumor T cell responses in the TMEs of our MC-38/B6 and CT26/BALB/c models by inhibiting H<sub>2</sub>O<sub>2</sub> production triggered by Th2/M2-related immunosuppression.

We also evaluated the role of VAP-1/AOC3 in human cancers. TCGA database analysis of various human cancers revealed that VAP-1/AOC3 expression was a negative prognostic factor in patients with colorectal, renal, and urothelial cancers. The relationship between VAP-1 and the response to checkpoint inhibitors remains to be evaluated. Significant positive correlations were observed of VAP-1 expression with the inferred activity of H<sub>2</sub>O<sub>2</sub> in the TME<sup>43</sup> and the expression of caveolin and Th2/M2-associated cytokines. In contrast, a negative correlation was observed between VAP-1 and IFN- $\gamma$  expression. Therefore, a similar VAP-1-driven immunosuppressive mechanism may be involved in some human cancers.

These results indicated that VAP-1 is involved in the generation of H<sub>2</sub>O<sub>2</sub>-mediated immunosuppressive Th2/M2 TMEs. U-V296 enhanced the anti-tumor activity of tumor antigen-specific CD8<sup>+</sup> T cells by improving such immunosuppressive TMEs. In addition, U-V296 exhibited significant synergistic anti-tumor effects with ICIs. Therefore, VAP-1 may be an attractive target for the development of combination cancer immunotherapy with ICIs.

## ACKNOWLEDGMENTS

This work was supported by Grants-in-Aid for Scientific Research from the Ministry of Education, Culture, Sports, Science and Technology (MEXT) of Japan (, 26221005, 15K09783, and 19K16808); the Project for Cancer Research And Therapeutic Evolution (P-CREATE) from Japan Agency for Medical Research and Development (AMED). We would like to thank Nobuo Tsukamoto, Yuki Katou, and Miyuki Saito for technical assistance and Misako Horikawa and Ryoko Suzuki for preparation of the manuscript.

## CONFLICTS OF INTEREST

Authors have no conflicts of interest to disclose.

## ORCID

Mohammad Abu Sayem  <https://orcid.org/0000-0001-9903-6959>

## REFERENCES

1. Wei SC, Duffy CR, Allison JP. Fundamental mechanisms of immune checkpoint blockade therapy. *Cancer Discov*. 2018;8:1069-1086.
2. Kawakami Y, Ohta S, Sayem MA, Tsukamoto N, Yaguchi T. Immune-resistant mechanisms in cancer immunotherapy. *Int J Clin Oncol*. 2020;25:810-817.
3. Knutson KL, Disis ML. Tumor antigen-specific T helper cells in cancer immunity and immunotherapy. *Cancer Immunol Immunother*. 2005;54:721-728.
4. Zhang Y, Choksi S, Chen K, Pobezinskaya Y, Linnoila I, Liu ZG. ROS play a critical role in the differentiation of alternatively activated macrophages and the occurrence of tumor-associated macrophages. *Cell Res*. 2013;23:898-914.
5. Spinelli JB, Yoon H, Ringel AE, Jeanfavre S, Clish CB, Haigis MC. Metabolic recycling of ammonia via glutamate dehydrogenase supports breast cancer biomass. *Science*. 2017;358:941-946.
6. Chen X, Song M, Zhang B, Zhang Y. Reactive oxygen species regulate T cell immune response in the tumor microenvironment. *Oxid Med Cell Longev*. 2016;2016:1580967.
7. Kono K, Salazar-Onfray F, Petersson M, et al. Hydrogen peroxide secreted by tumor-derived macrophages down-modulates signal-transducing zeta molecules and inhibits tumor-specific T cell-and natural killer cell-mediated cytotoxicity. *Eur J Immunol*. 1996;26:1308-1313.
8. Salmi M, Jalkanen S. Vascular adhesion protein-1: a cell surface amine oxidase in translation. *Antioxid Redox Signal*. 2019;30(3):314-332. <http://doi.org/10.1089/ars.2017.7418>
9. Bonder CS, Norman MU, Swain MG, et al. Rules of recruitment for Th1 and Th2 lymphocytes in inflamed liver: a role for alpha-4 integrin and vascular adhesion protein-1. *Immunity*. 2005;23:153-163.
10. Shetty S, Weston CJ, Oo YH, et al. Common lymphatic endothelial and vascular endothelial receptor-1 mediates the transmigration of regulatory T cells across human hepatic sinusoidal endothelium. *J Immunol*. 2011;186:4147-4155.
11. Aspinall AI, Curbishley SM, Lalor PF, et al. CX(3)CR1 and vascular adhesion protein-1-dependent recruitment of CD16(+)

- monocytes across human liver sinusoidal endothelium. *Hepatology*. 2010;51:2030-2039.
12. Weston CJ, Shepherd EL, Claridge LC, et al. Vascular adhesion protein-1 promotes liver inflammation and drives hepatic fibrosis. *J Clin Invest*. 2015;125:501-520.
  13. Salmi M, Jalkanen S. Cell-surface enzymes in control of leukocyte trafficking. *Nat Rev Immunol*. 2005;5:760-771.
  14. Kivi E, Elima K, Aalto K, et al. Human Siglec-10 can bind to vascular adhesion protein-1 and serves as its substrate. *Blood*. 2009;114:5385-5392.
  15. Molinier-Frenkel V, Castellano F. Immunosuppressive enzymes in the tumor microenvironment. *FEBS Lett*. 2017;591:3135-3157.
  16. Luo C, Shen G, Liu N, et al. Ammonia drives dendritic cells into dysfunction. *J Immunol*. 2014;193:1080-1089.
  17. Targowski SP, Klucinski W, Babiker S, Nonnecke BJ. Effect of ammonia on in vivo and in vitro immune responses. *Infect Immun*. 1984;43:289-293.
  18. Moser H. Electrophysiological evidence for ammonium as a substitute for potassium in activating the sodium pump in a crayfish sensory neuron. *Can J Physiol Pharmacol*. 1987;65:141-145.
  19. Bosoi CR, Rose CF. Identifying the direct effects of ammonia on the brain. *Metab Brain Dis*. 2009;24:95-102.
  20. Fiaschi T, Chiarugi P. Oxidative stress, tumor microenvironment, and metabolic reprogramming: a diabolic liaison. *Int J Cell Biol*. 2012;2012:762825.
  21. Kim YW, Byzova TV. Oxidative stress in angiogenesis and vascular disease. *Blood*. 2014;123:625-631.
  22. Parola M, Robino G. Oxidative stress-related molecules and liver fibrosis. *J Hepatol*. 2001;35:297-306.
  23. Frossi B, De Carli M, Piemonte R, Pucillo C. Oxidative microenvironment exerts an opposite regulatory effect on cytokine production by Th1 and Th2 cells. *Mol Immunol*. 2008;45:58-64.
  24. Obata F, Hoshino A, Toyama A. Hydrogen peroxide increases interleukin-12 p40/p70 molecular ratio and induces Th2-predominant responses in mice. *Scand J Immunol*. 2006;63:125-130.
  25. Nakao S, Noda K, Zandi S, et al. VAP-1-mediated M2 macrophage infiltration underlies IL-1 $\beta$ - but not VEGF-A-induced lymph- and angiogenesis. *Am J Pathol*. 2011;178:1913-1921.
  26. Schmielau J, Finn OJ. Activated granulocytes and granulocyte-derived hydrogen peroxide are the underlying mechanism of suppression of t-cell function in advanced cancer patients. *Cancer Res*. 2001;61:4756-4760.
  27. Otsuji M, Kimura Y, Aoe T, Okamoto Y, Saito T. Oxidative stress by tumor-derived macrophages suppresses the expression of CD3 zeta chain of T-cell receptor complex and antigen-specific T-cell responses. *Proc Natl Acad Sci U S A*. 1996;93:13119-13124.
  28. Vainio PJ, Kortekangas-Savolainen O, Mikkola JH, et al. Safety of blocking vascular adhesion protein-1 in patients with contact dermatitis. *Basic Clin Pharmacol Toxicol*. 2005;96:429-435.
  29. O'Rourke AM, Wang EY, Salter-Cid L, et al. Benefit of inhibiting SSOA in relapsing experimental autoimmune encephalomyelitis. *J Neural Transm (Vienna)*. 2007;114:845-849.
  30. Pannecoeck R, Serruys D, Benmeridja L, et al. Vascular adhesion protein-1: Role in human pathology and application as a biomarker. *Crit Rev Clin Lab Sci*. 2015;52:284-300.
  31. Marttila-Ichihara F, Auvinen K, Elima K, Jalkanen S, Salmi M. Vascular adhesion protein-1 enhances tumor growth by supporting recruitment of Gr-1+CD11b+ myeloid cells into tumors. *Cancer Res*. 2009;69:7875-7883.
  32. Marttila-Ichihara F, Castermans K, Auvinen K, et al. Small-molecule inhibitors of vascular adhesion protein-1 reduce the accumulation of myeloid cells into tumors and attenuate tumor growth in mice. *J Immunol*. 2010;184:3164-3173.
  33. Yoong KF, McNab G, Hübscher SG, Adams DH. Vascular adhesion protein-1 and ICAM-1 support the adhesion of tumor-infiltrating lymphocytes to tumor endothelium in human hepatocellular carcinoma. *J Immunol*. 1998;160:3978-3988.
  34. Irjala H, Salmi M, Alanen K, Grénman R, Jalkanen S. Vascular adhesion protein 1 mediates binding of immunotherapeutic effector cells to tumor endothelium. *J Immunol*. 2001;166:6937-6943.
  35. Forster-Horváth C, Döme B, Paku S, et al. Loss of vascular adhesion protein-1 expression in intratumoral microvessels of human skin melanoma. *Melanoma Res*. 2004;14:135-140.
  36. Yaguchi T, Kobayashi A, Inozume T, et al. Human PBMC-transferred murine MHC class I/II-deficient NOG mice enable long-term evaluation of human immune responses. *Cell Mol Immunol*. 2018;15:953-962.
  37. Medina I, Carbonell J, Pulido L, et al. Babelomics: an integrative platform for the analysis of transcriptomics, proteomics and genomic data with advanced functional profiling. *Nucleic Acids Res*. 2010;38:W210-213.
  38. Newman AM, Liu CL, Green MR, et al. Robust enumeration of cell subsets from tissue expression profiles. *Nat Methods*. 2015;12:453-457.
  39. Chen Z, Huang A, Sun J, Jiang T, Qin FX, Wu A. Inference of immune cell composition on the expression profiles of mouse tissue. *Sci Rep*. 2017;7:40508.
  40. Mohanty JG, Jaffe JS, Schulman ES, Raible DG. A highly sensitive fluorescent micro-assay of H<sub>2</sub>O<sub>2</sub> release from activated human leukocytes using a dihydroxyphenoxazine derivative. *J Immunol Methods*. 1997;202:133-141.
  41. Takashi S, Akihiko Y. In vitro Th differentiation protocol. In: Feng X-H, Xu P, Lin X, eds. *TGF- $\beta$  Signaling*. Clifton, NJ: Humana Press, New York, NY, 2015; 183-191.
  42. Dudley ME, Wunderlich JR, Shelton TE, Even J, Rosenberg SA. Generation of tumor-infiltrating lymphocyte cultures for use in adoptive transfer therapy for melanoma patients. *J Immunother*. 2003;26:332-342.
  43. Volonte D, Zhang K, Lisanti MP, Galbiati F. Expression of caveolin-1 induces premature cellular senescence in primary cultures of murine fibroblasts. *Mol Biol Cell*. 2002;13:2502-2517.
  44. Sartoretto JL, Kalwa H, Pluth MD, Lippard SJ, Michel T. Hydrogen peroxide differentially modulates cardiac myocyte nitric oxide synthesis. *Proc Natl Acad Sci U S A*. 2011;108:15792-15797.
  45. Satoh T, Takeuchi O, Vandenbon A, et al. The Jmjd3-Irf4 axis regulates M2 macrophage polarization and host responses against helminth infection. *Nat Immunol*. 2010;11:936-944.
  46. Chen DB, Li SM, Qian XX, Moon C, Zheng J. Tyrosine phosphorylation of caveolin 1 by oxidative stress is reversible and dependent on the c-src tyrosine kinase but not mitogen-activated protein kinase pathways in placental artery endothelial cells. *Biol Reprod*. 2005;73:761-772.
  47. Frossi B, De Carli M, Daniel KC, Rivera J, Pucillo C. Oxidative stress stimulates IL-4 and IL-6 production in mast cells by an APE/Ref-1-dependent pathway. *Eur J Immunol*. 2003;33:2168-2177.
  48. Casero RA, Murray Stewart T, Pegg AE. Polyamine metabolism and cancer: treatments, challenges and opportunities. *Nat Rev Cancer*. 2018;18:681-695.

## SUPPORTING INFORMATION

Additional supporting information may be found online in the Supporting Information section.

**How to cite this article:** Kinoshita T, Sayem MA, Yaguchi T, et al. Inhibition of vascular adhesion protein-1 enhances the anti-tumor effects of immune checkpoint inhibitors. *Cancer Sci*. 2021;112:1390-1401. <https://doi.org/10.1111/cas.14812>